VIP The following Communications have been judged by at least two referees to be "very important papers" and will be published online at www.angewandte.org soon:

*H. Chinen, K. Mawatari, Y. Pihosh, K. Morikawa, Y. Kazoe, T. Tsukahara, T. Kitamori**
Enhancement of Proton Mobility in Extended Nanospace Channels*A. Patzer, M. Schütz, T. Möller, O. Dopfer**
IR Spectrum and Structure of the Adamantane Cation: Direct Evidence for Jahn–Teller Distortion

*C. Giese, F. Zosel, C. Puorger, R. Glockshuber**
The Most Stable Protein/Ligand Complex: Applications for One-Step Affinity Purification and Identification of Protein Assemblies

*C. Lux, M. Wollenhaupt, T. Bolze, Q. Liang, J. Köhler, C. Sarpe, T. Baumert**
Circular Dichroism in the Photoelectron Angular Distributions of Camphor and Fenchone from Multiphoton Ionization with Femtosecond Laser Pulses

*X.-F. Xiong, Q. Zhou, J. Gu, L. Dong, T.-Y. Liu, Y.-C. Chen**
Trienamine Catalysis of 2,4-Dienones: Development and Application in Asymmetric Diels–Alder Reaction

M. T. C. Walvoort, H. Van den Elst, O. J. Plante, L. Kröck, P. H. Seeberger, H. S. Overkleeft, G. A. van der Marel, J. D. Codée**
Automated Solid-Phase Synthesis of β-Mannuronic Acid Alginates

*P. G. Schiro, M. Zhao, J. S. Kuo, K. M. Koehler, D. E. Sabath, D. T. Chiu**
Sensitive and High-Throughput Isolation of Rare Cells from Peripheral Blood with Ensemble-Decision Aliquot Ranking

*H. Ding, A. G. Roberts, P. G. Harran**
Synthetic (±)-Axinellamines Deficient in Halogen

*J. Lu, C. Aydin, N. D. Browning, B. C. Gates**
Imaging Gold Atom Catalytic Sites in Zeolite NaY

Author Profile

"I would have liked to have discovered the triphenylmethyl radical.
My favorite food is fondue. …"
This and more about Armido Studer can be found on page 4000.

News


D. Seidel


J. Hartig


M. Mann


P. Bruce


J. A. Lercher

Books

Highlights

Tissue Engineering

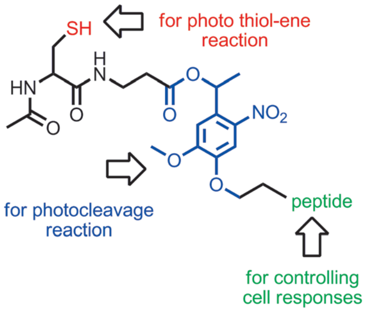

Click, click, and lights on: A new generation of biomaterials for use as cell-supporting scaffolds includes added features to mimic the natural temporal and spatial control of bioactive ligands. The reported system uses one cycle to add and remove biorelevant ligands, which is a step towards representing the dynamic progression of natural organ and tissue development.

Molecular Shuttles

A new door is open! Foldamers have been successfully utilized for the development of a molecular device. Termed foldaxanes by analogy with rotaxanes, these structures are formed through a multitude of noncovalent interactions between double-helical foldamers and rod-shaped guest molecules. The foldaxanes move in a screw-type motion and open up yet another promising application of foldamers in materials science.

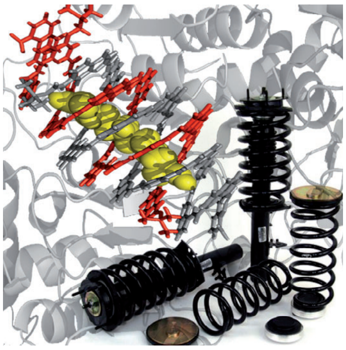

Natural Products

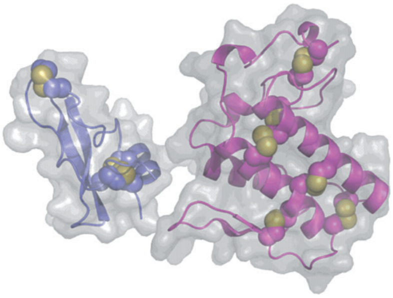

Gaining on pain: Two snake protein toxins combine to form a heteromeric complex, MitTx, which activates acid-sensing ion channels (ASICs) and elicits pain. MitTx is used to explore the roles of specific ASIC subtypes in pain pathways. These insights may provide new pharmacological tools ultimately leading to new treatments for pain.

For the USA and Canada:
ANGEWANDTE CHEMIE International Edition (ISSN 1433-7851) is published weekly by Wiley-VCH, PO Box 191161, 69451 Weinheim, Germany. Air freight and mailing in the USA by Publications Expediting Inc., 200 Meacham Ave., Elmont, NY 11003. Periodicals postage paid at Jamaica, NY 11431. US POSTMASTER: send address changes to *Angewandte Chemie*, Journal Customer Services, John Wiley & Sons Inc., 350 Main St., Malden, MA 02148-5020. Annual subscription price for institutions: US$ 11.738/10.206 (valid for print and electronic / print or electronic delivery); for individuals who are personal members of a national chemical society prices are available on request. Postage and handling charges included. All prices are subject to local VAT/sales tax.

Minireviews

Total Synthesis

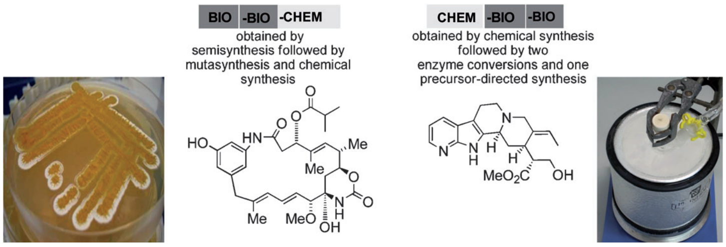

Taking it easy: Natural product synthesis is a stressful task. Exploiting the understanding of biosynthetic pathways and implementing genetic engineering into the synthetic chemist's portfolio paves the way for new alternatives for natural product synthesis. This Minireview describes “hybrid” strategies of organic synthesis and biosynthesis that result in facile access to complex natural products and libraries based on them.

Reviews

Antivirulence Agents

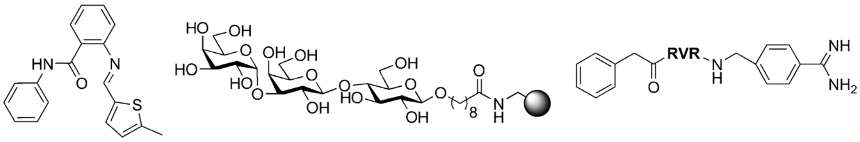

The overuse of antibiotics for the treatment of bacterial infections leads to serious problems such as the development of resistant strains. In alternative approaches, the action of bacterial toxins is inhibited as a means to treat diseases caused by toxin-producing bacteria.

Communications

Antibiotic Biosynthesis

VIP

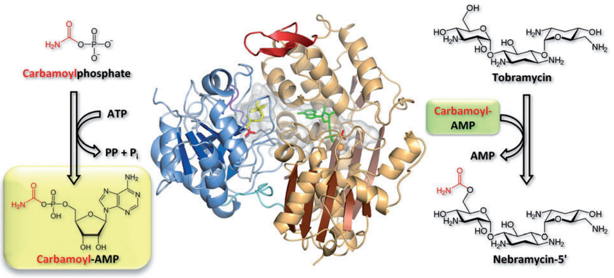

An ancient reaction vessel: TobZ carbamoylates the antibiotic tobramycin to form nebramycin 5′. The YrdC-like domain (blue) catalyzes the formation of the novel intermediate carbamoyladenylate, which is channeled through a common “reaction chamber” to the Kae1-like domain (brown), site of carbamoyl transfer.

Terpene Biosynthesis

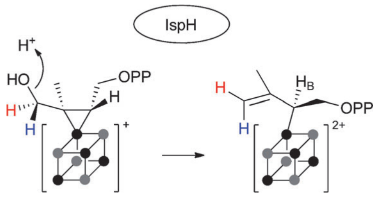

On the right path: The stereochemcial course of the IspH reaction, the last reaction in the deoxyxylulose phosphate pathway to terpenes, was investigated in feeding experiments with deuterated isotopologues of 1-deoxy-D-xylulose. The results support an enzyme mechanism for IspH that involves a previously suggested metallacyclopropane intermediate.

Bioactive Non-Native Peptides

The one and only fold? Three chemically synthesized μ-conotoxin PIIIA isomers (see picture), which contain different disulfide connectivity, block the skeletal muscle voltage-gated sodium channel Na_V1.4 with similar, yet distinguishable potency. Hence, bioactivity of this μ-conotoxin is not strictly coupled to its native fold. Future development of conotoxin-derived analgesics may benefit from such a widened structural repertoire.

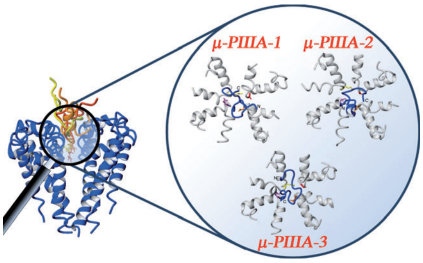

Stereoselective Photocatalysis

Dream team: Heterogeneous inorganic semiconductors and chiral organocatalysts team up for the stereoselective photocatalytic formation of carbon–carbon bonds. However, the connection between the organic and inorganic catalysts should not be too tight: Covalent immobilization inactivates the system.

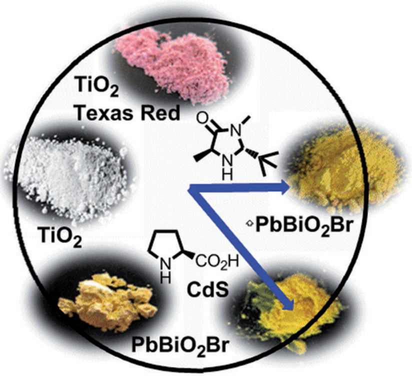

Hydrogen Bonds in DNA i-Motifs

Give and take: Combined NMR spectroscopic and quantum chemical investigations are used to characterize cationic hydrogen bonds found in $C{\cdot}C^+$ base pairs in DNA i-motif structures. The proton involved in the singly protonated base pair jumps between both cytidine nucleobases (see picture). The proton transfer can be described as asymmetric double-well potential with a proton hopping rate of at least 10^8 s^{-1}.

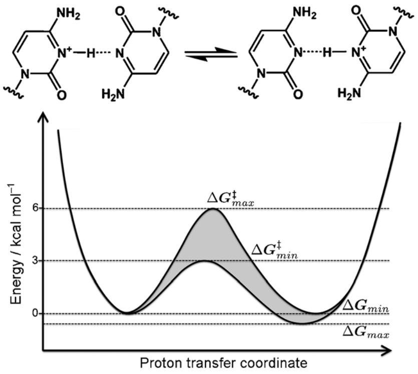

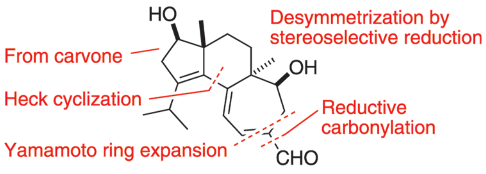

Cyrneine A

Neuritogenic natural products: The tricyclic diterpene cyrneine A featuring a hexatrienal unit was prepared synthetically for the first time by a Heck reaction, a carbene ring expansion, and a reductive carbonylation. The structure of the natural product was assigned by X-ray crystal analysis of a synthetic sample.

Natural Product Synthesis

E. Elamparuthi, C. Fellay, M. Neuburger, K. Gademann* ________ **4071 – 4073**

Total Synthesis of Cyrneine A

Live wire: Thermal decomposition of β-FeOOH nanowires at 550 °C in an oxygen-deficient atmosphere generates highly photoactive hematite nanowires (N-hematite), which yielded a substantially enhanced photocurrent density, as compared to a hematite sample prepared in air (A-hematite). This enhanced photoactivity is attributed to the improved donor density of hematite nanowires, as a result of formation of oxygen vacancies.

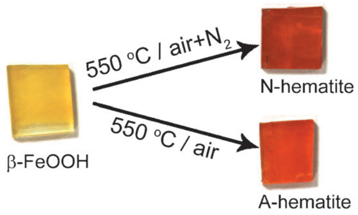

Photochemistry

Y. Ling, G. Wang, J. Reddy, C. Wang, J. Z. Zhang, Y. Li* ________ **4074 – 4079**

The Influence of Oxygen Content on the Thermal Activation of Hematite Nanowires

---

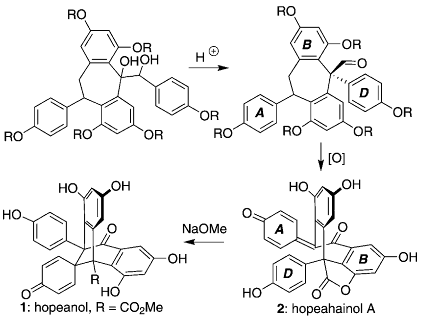

Rearranging complexity: The total synthesis of resveratrol dimers hopeanol (**1**) and hopeahainol A (**2**, see scheme) is described. By using a reagent-driven pinacol rearrangement coupled with specific oxidation chemistry, the frameworks are constructed concisely and on scale. Moreover, the route has biogenetic implications that trace the origin of these compounds to more common dimeric family members.

Natural Products

S. A. Snyder,* S. B. Thomas, A. C. Mayer, S. P. Breazzano ________ **4080 – 4084**

Total Syntheses of Hopeanol and Hopeahainol A Empowered by a Chiral Brønsted Acid Induced Pinacol Rearrangement

---

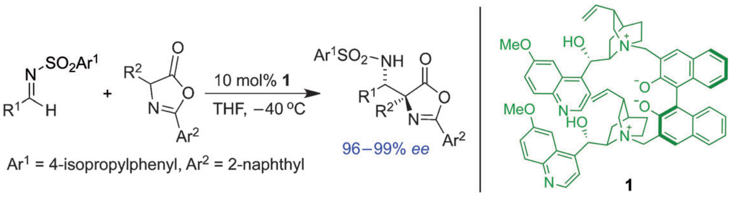

By design: New chiral bis(betaine)s, for example **1**, containing two catalytically active centers have been designed. They have proven to be promising organocatalysts for the direct Mannich-type reaction of azlactones with a broad spectrum of aliphatic imines, thus affording α-tetrasubstituted α,β-diamino acid surrogates with excellent enantioselectivities.

Organocatalysis

W.-Q. Zhang, L.-F. Cheng, J. Yu, L.-Z. Gong* ________ **4085 – 4088**

A Chiral Bis(betaine) Catalyst for the Mannich Reaction of Azlactones and Aliphatic Imines

Thin Films

L. Li, X. Shen, S. W. Hong, R. C. Hayward,*
T. P. Russell* ________ 4089 – 4094

Fabrication of Co-continuous Nanostructured and Porous Polymer Membranes: Spinodal Decomposition of Homopolymer and Random Copolymer Blends

Scale down: Thin films with co-continuous morphologies are fabricated with characteristic length scales, down to tens of nanometers, based on the phase separation of a polymer blend. The degree of immiscibility between polystyrene and poly(2-vinylpyridine) was tuned to mediate nonfavorable interactions between the two components. The co-continuous structured films provide templates for thin nanoporous membranes (see images).

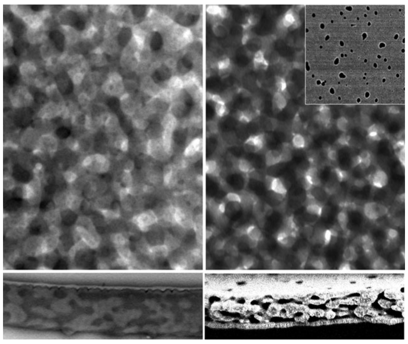

Materials Science

M. Shimizu,* R. Kaki, Y. Takeda,
T. Hiyama, N. Nagai, H. Yamagishi,
H. Furutani ________ 4095 – 4099

1,4-Bis(diarylamino)-2,5-bis(4-cyanophenylethenyl)benzenes: Fluorophores Exhibiting Efficient Red and Near-Infrared Emissions in Solid State

Molecular fluorophores of type A–π–D–π–A (D = donor, A = acceptor) demonstrate solid-state emission in the red to near-infrared region with high efficiency. The emission color can be tuned through the substituents on the diarylamino and cyanophenyl moieties. The electroluminescence performance of the designed fluorophore confirms its potential as an emitter for use in organic light-emitting devices.

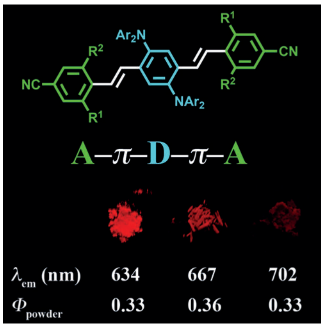

Metal-Ion Sensors

N. Kotera, N. Tassali, E. Léonce, C. Boutin,
P. Berthault,* T. Brotin, J. P. Dutasta,
L. Delacour, T. Traoré, D. A. Buisson,
F. Taran, S. Coudert,
B. Rousseau* ________ 4100 – 4103

A Sensitive Zinc-Activated ^{129}Xe MRI Probe

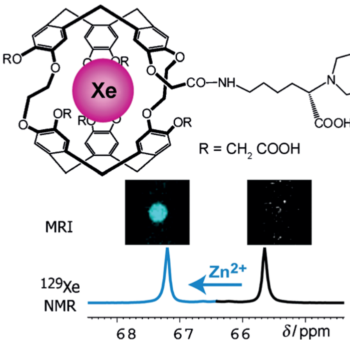

Xenon capsule: A smart ^{129}Xe NMR-based sensor of Zn^{2+} ions for magnetic resonance imaging (MRI) is proposed. The resonance frequency of xenon encapsulated in a cryptophane that bears a nitrilotriacetic ligand moiety varies when Zn^{2+} ions are present in solution (see picture). With hyper-polarized gas, such a construct enables detection of 100 nM zinc in one xenon batch, a threshold 300 times lower than achieved with gadolinium chelates.

Organocatalysis

G. Talavera, E. Reyes, J. L. Vicario,*
L. Carrillo ________ 4104 – 4107

Cooperative Dienamine/Hydrogen-Bonding Catalysis: Enantioselective Formal [2+2] Cycloaddition of Enals with Nitroalkenes

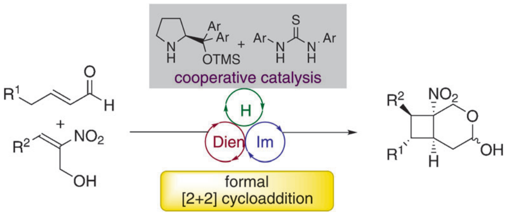

Two can play this game: The title reaction is catalyzed by a chiral secondary amine in the presence of an achiral thiourea for the enantio- and diastereoselective synthesis of highly functionalized cyclobutanes (see scheme; TMS = trimethylsilyl). Mechanistically, two consecutive Michael reactions proceed through an unprecedented combination of an dienamine/iminium activation mode.

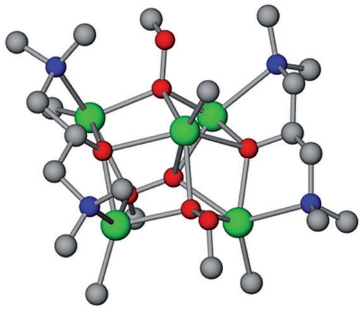

Cadmium burning: The violent reaction of $CdMe_2$ with O_2 has been controlled by the use of a cadmium aminoalkoxide supporting ligand. The first examples of cadmium organoperoxides, arising from O_2 insertion into the Cd–C bond, are thus formed (see picture; Cd green, C gray, N blue, O red).

Cadmium Peroxides

A. L. Johnson, N. Hollingsworth,
G. Kociok-Köhn,
K. C. Molloy* ——— **4108–4111**

O_2 Insertion into a Cadmium–Carbon Bond: Structural Characterization of Organocadmium Peroxides

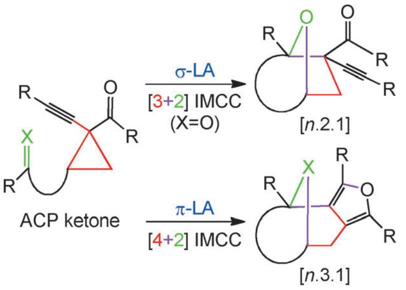

One brick, two bridges: The choice of the catalyzing Lewis acid (LA, π: π-electrophilic, σ: σ-electrophilic) determines the pathway ([4+2] or [3+2]) of catalytic intramolecular cycloaddition reactions (IMCCs) of alkynylcyclopropane (ACP) ketone. This method provides a general strategy for stereoselective construction of structurally diverse bridged oxa-/aza-[*n*.3.1] and oxa-/aza-[*n*.2.1] skeletons (see scheme).

Cycloadditions

Y. Bai, W. Tao, J. Ren,
Z. Wang* ——— **4112–4116**

Lewis Acid Catalyzed Intramolecular [4+2] and [3+2] Cross-Cycloaddition of Alkynylcyclopropane Ketones with Carbonyl Compounds and Imines

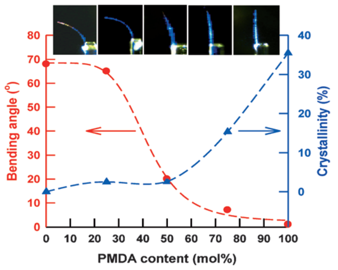

Bending the rules: The role of crystallinity in the generation of photomechanical effects is examined for a series of linear azobenzene-functionalized polyimides. The less pyromellitic dianhydride (PMDA) that is present in the polyimide the less crystalline it is, and therefore the more the cantilever bends when exposed to light (see figure).

Azo Compounds

K. M. Lee, D. H. Wang, H. Koerner,
R. A. Vaia, L.-S. Tan,*
T. J. White* ——— **4117–4121**

Enhancement of Photogenerated Mechanical Force in Azobenzene-Functionalized Polyimides

Copper-catalyzed allylic alkylation of azoles, a pyridine *N*-oxide, and fluoroarenes with secondary allylic phosphates proceeded under mild reaction conditions with excellent γ-*E*-selectivity. The reactions with enantioenriched allylic phosphates proceeded with 1,3-*anti* stereoselectivity to generate an allylic stereogenic center at the position α to the aromatic ring.

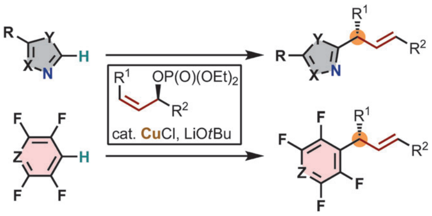

Allylic Alkylation

Y. Makida, H. Ohmiya,*
M. Sawamura* ——— **4122–4127**

Regio- and Stereocontrolled Introduction of Secondary Alkyl Groups to Electron-Deficient Arenes through Copper-Catalyzed Allylic Alkylation

Alkaloid Synthesis

N. R. Babij, J. P. Wolfe* ____ **4128 – 4130**

Asymmetric Total Synthesis of (+)-Merobatzelladine B

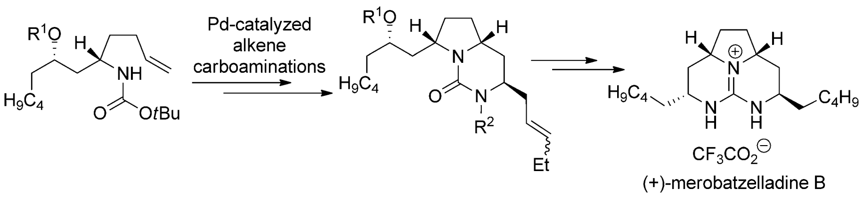

Putting the *syn* in synthesis: The first total synthesis of (+)-merobatzelladine B was accomplished using an iterative sequence of stereoselective palladium-catalyzed alkene carboamination reactions for formation of two of the three rings. This represents a new strategy for the generation of polycyclic guanidine natural products, and provides access to compounds with a *syn* relationship between the C6 hydrogen atom and the C8 alkyl group.

Homogeneous Catalysis

S. Suzuki, E. Tokunaga, D. S. Reddy, T. Matsumoto, M. Shiro, N. Shibata* ____ **4131 – 4135**

Enantioselective 5-*endo*-dig Carbocyclization of β-Ketoesters with Internal Alkynes Employing a Four-Component Catalyst System

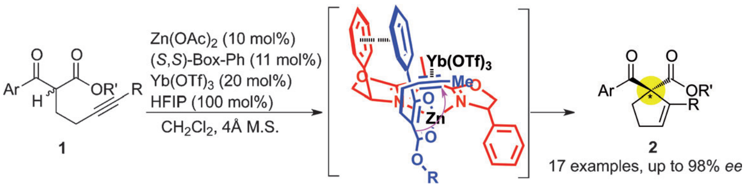

It takes four: The title reaction was achieved for the first time by employing a four-component catalyst system, Zn^{II}/Box-Ph/$Yb(OTf)_3$/HFIP, to deliver the products in high yields and enantioselectivities. Fluorination of one of the products with Selectfluor provides a medicinally attractive allylic fluoride in good yield. Box-Ph = 2,2′-isopropylidine bis(4-phenyl-2-oxazoline), HFIP = hexafluoroisopropyl alcohol.

Asymmetric Hydrogenation

VIP

R. Kuwano,* R. Morioka, M. Kashiwabara, N. Kameyama ____ **4136 – 4139**

Catalytic Asymmetric Hydrogenation of Naphthalenes

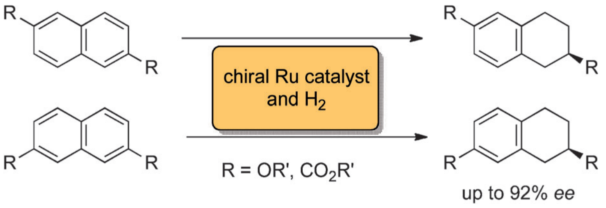

Vanishing aromaticity: A chiral ruthenium complex catalyzes the hydrogenation of 2,6- or 2,7-disubstituted naphthalenes to give chiral tetralins with up to 92% *ee*. The chiral catalyst is applicable to the regio- and enantioselective reduction of 6-substituted 2-alkoxynaphthalenes and preferentially hydrogenates the alkoxy-substituted arene rings.

Photochemistry

R. S. Andrews, J. J. Becker, M. R. Gagné* ____ **4140 – 4143**

A Photoflow Reactor for the Continuous Photoredox-Mediated Synthesis of *C*-Glycoamino Acids and *C*-Glycolipids

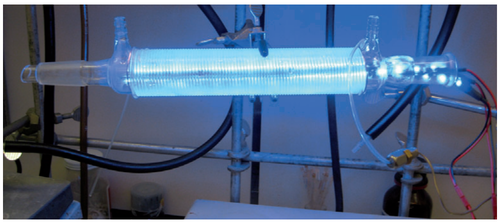

Go with the flow: A simple flow reactor has been developed to accommodate highly absorbing $[RuL_3]^{2+}$ photosensitizers for light-starved photoredox reactions (see picture). The use of vessels having a thin diameter increases the efficiency of the reaction. This methodology has been applied to the divergent synthesis of *C*-glycoconjugates.

Photochemistry

J. W. Tucker, Y. Zhang, T. F. Jamison, C. R. J. Stephenson* ______ **4144 – 4147**

Visible-Light Photoredox Catalysis in Flow

Photoredox catalysis: A variety of organic transformations mediated by visible-light-active photoredox catalysts have been conducted in a photochemical flow reactor. The reactor design is very simple and can be easily implemented in any laboratory (see picture). In addition, this reactor afforded a marked increase in the reaction rate compared to those observed in typical batch (round bottom flask) reactors.

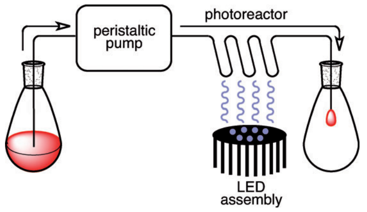

Fluorescent Probes

T. Yoshihara, Y. Yamaguchi, M. Hosaka, T. Takeuchi, S. Tobita* _____ **4148 – 4151**

Ratiometric Molecular Sensor for Monitoring Oxygen Levels in Living Cells

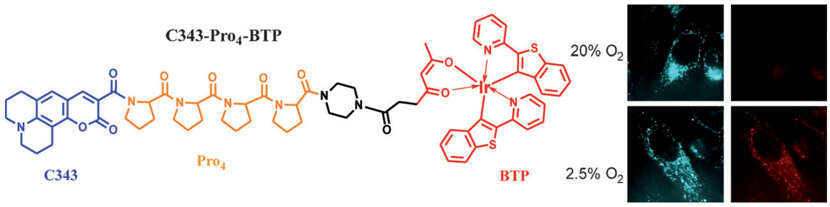

A ratiometric oxygen sensor (C343-Pro$_4$-BTP) that uses coumarin 343 (blue in picture) as an oxygen-insensitive fluorophore and an iridium complex (BTP, red in picture) as an oxygen-sensitive phosphor can be used to determine the oxygen concentration in solution and in living cells, which was demonstrated by ratiometric measurements of the blue coumarin 343 fluorescence and the red BTP phosphorescence in C343-Pro$_4$-BTP (see picture).

Concerted Dehydrogenation

L. Roy, S. Mittal, A. Paul* __ **4152 – 4156**

Breaking the Myth of the Recalcitrant Chemisorbed Hydrogens on Boron Niride Nanotubes: A Theoretical Perspective

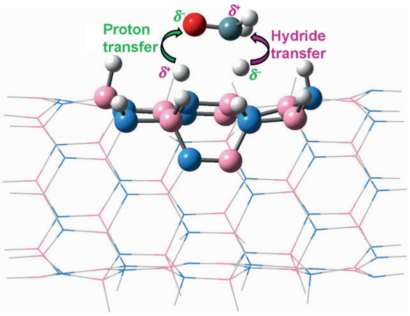

Chemical hydrogen storage: Theoretical investigations showed that the dehydrogenation of chemisorbed hydrogen atoms on boron nitride nanotubes (BNNT) could be triggered by appropriate reagents through simultaneous proton and hydride transfer (see picture). The computed free-energy of the activation barrier for the reduction of formaldehyde to methanol by chemisorbed hydrogen atoms on a zigzag BNNT was predicted to be 12.7 kcal mol^{-1} in THF.

Enzyme Mechanisms

F. Ren, T.-P. Ko, X. Feng, C.-H. Huang, H.-C. Chan, Y. Hu, K. Wang, Y. Ma, P.-H. Liang, A. H.-J. Wang, E. Oldfield,* R.-T. Guo* ____________ **4157 – 4160**

Insights into the Mechanism of the Antibiotic-Synthesizing Enzyme MoeO5 from Crystal Structures of Different Complexes

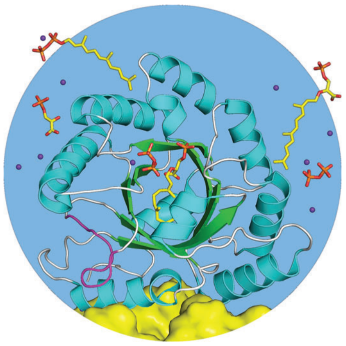

Barrel-shaped: The enzyme MoeO5 catalyzes the transfer of the C$_{15}$ moiety of farnesyl pyrophosphate to the 2-hydroxy group of 3-phosphoglycerate to give 2-(*Z*,*E*)-farnesyl-3-phosphoglycerate (FPG; ligand in the center of the shown structure). X-ray crystallographic structures showed that MoeO5 forms a triose-phosphate-isomerase barrel structure and binds FPG in a curved pocket, mainly as a result of its long λ3 loop (magenta in picture).

Back Cover

Protein Chemistry

J. E. Hudak, R. M. Barfield, G. W. de Hart, P. Grob, E. Nogales, C. R. Bertozzi,* D. Rabuka* ______ **4161 – 4165**

Synthesis of Heterobifunctional Protein Fusions Using Copper-Free Click Chemistry and the Aldehyde Tag

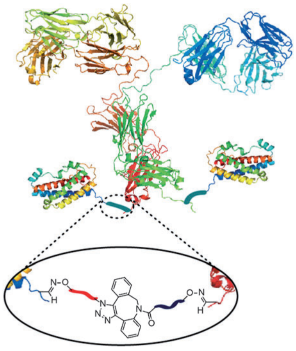

Clicking into place: Cu-free click chemistry is combined with the aldehyde tag protein modification strategy to produce heterobifunctional protein fusions. This method relies on linkers that utilize orthogonal triazole and oxime chemistries (see scheme) to expand on conjugation with the fGly residue and enables site-specific protein conjugation to full-length human antibodies.

Protein Labeling

T. Plass, S. Milles, C. Koehler, J. Szymański, R. Mueller, M. Wießler, C. Schultz,* E. A. Lemke* __ **4166 – 4170**

Amino Acids for Diels–Alder Reactions in Living Cells

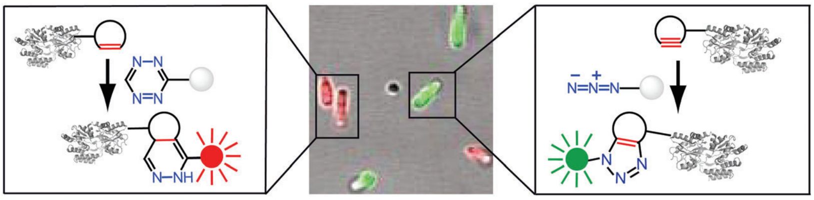

Under tension: A set of genetically encoded unnatural amino acids can be used for biocompatible site-specific labeling of proteins with fluorogenic dyes. The new compounds have norbornene and *trans*-cyclooctene units that react with tetrazine derivatives in an inverse-electron-demand Diels–Alder cycloaddition (left in picture). The technique offers fast labeling that is orthogonal to labeling through azide–cyclooctyne click reaction (right).

Drug Design

R. Jørgensen, L. L. Grimm, N. Sindhuwinata, T. Peters, M. M. Palcic* ______ **4171 – 4175**

A Glycosyltransferase Inhibitor from a Molecular Fragment Library Simultaneously Interferes with Metal Ion and Substrate Binding

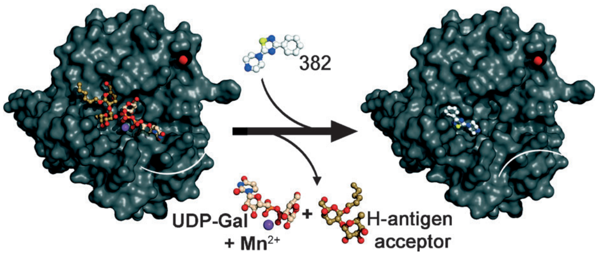

A fragmented approach: 3-Phenyl-5-piperazino-1,2,4-thiadiazole (designated “compound 382” in the Ro5 Maybridge Fragment Library, see scheme) is demonstrated to be an effective inhibitor of human blood group glycosyltransferase B. The compound interferes with both acceptor and donor binding and also displaces the Mn^{2+} ion in the binding pocket.

Surface Science

Y. Zhu, Q. Wang, L. Zhao, Y. Han* ______ **4176 – 4180**

Direct Observation of Surface Reconstruction and Termination on a Complex Metal Oxide Catalyst by Electron Microscopy

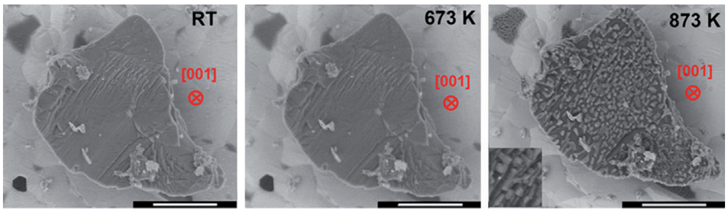

On the surface: The surface reconstruction of an MoVTeO complex metal oxide catalyst was observed directly by various electron microscopic techniques and the results explain the puzzling catalytic behavior.

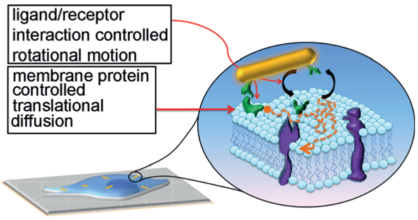

Track changes: A robust high-speed and high-precision single nanoparticle translational and rotational tracking method has been developed to directly monitor the interactions between transferrin-modified nanocargos (gold nanorods) and the membrane proteins prior to endocytosis (see picture). This approach shows that the translational and rotational diffusions of nanocargos on living cell membranes are unsynchronized in space and in time.

Nanocargo Diffusion

L. Xiao, L. Wei, C. Liu, Y. He,
E. S. Yeung* ________ **4181 – 4184**

Unsynchronized Translational and Rotational Diffusion of Nanocargo on a Living Cell Membrane

---

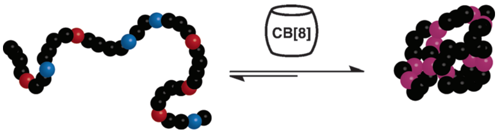

Smart materials: Metastable single-chain polymeric nanoparticles were prepared through stimuli-responsive and reversible intramolecular crosslinking of a single polymer chain in water. Functionalization of poly(*N*-hydroxyethylacrylamide) polymers with two complementary guests for cucurbit[8]uril (CB[8]), namely viologen and naphthalene, followed by addition of the macrocycle thus allowed for facile preparation of such nanoparticles (see picture).

Folding of Polymer Chains

E. A. Appel, J. Dyson, J. del Barrio,
Z. Walsh, O. A. Scherman* _ **4185 – 4189**

Formation of Single-Chain Polymer Nanoparticles in Water through Host–Guest Interactions

---

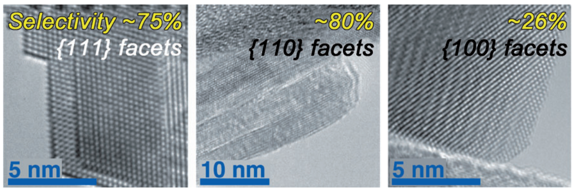

Catalyst design: First principles calculations predict that phosgene can be substituted by dimethyl carbonate (DMC) in the carbamoylation of aromatic amines when using a CeO_2 catalyst preferentially exposing the low energy {111} facet. Experimental results confirm the theoretical predictions, and CeO_2 nano-octahedra terminated by low energy {111} facets show high activity and selectivity toward the desired dicarbamoylated product.

CeO_2 Nanocatalysts

S. Laursen, D. Combita, A. B. Hungría,
M. Boronat, A. Corma* ____ **4190 – 4193**

First-Principles Design of Highly Active and Selective Catalysts for Phosgene-Free Synthesis of Aromatic Polyurethanes

---

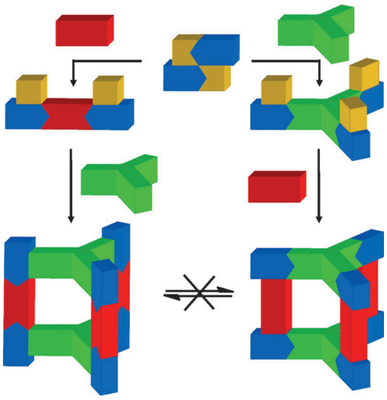

In control: Multicomponent stereoisomeric assemblies have been synthesized from asymmetric cyclometalated platinum corner units that have exchangeable *cis* coordination sites with different labilities. A template-free, kinetically controlled approach resulted in the selective formation of trigonal prismatic isomers by changing the sequence of addition of 4,4′-bipyridine (red) and tris(4-pyridyl)triazine (green) to $[(\mathbf{L}Pt)_2Cl_2]$ (blue and yellow; H**L** = 2-phenylpyridine).

Self-Assembly

VIP

O. Chepelin, J. Ujma, P. E. Barran,*
P. J. Lusby* ________ **4194 – 4197**

Sequential, Kinetically Controlled Synthesis of Multicomponent Stereoisomeric Assemblies

Inside Cover

Single-Atom Catalysis

Z. Huang, X. Gu, Q. Cao, P. Hu, J. Hao, J. Li,* X. Tang* ______ **4198 – 4203**

Catalytically Active Single-Atom Sites Fabricated from Silver Particles

Silver chains fabricated from supported silver particles were embedded in Hollandite-type manganese oxide, thereby exposing single silver atoms as catalytically active sites (see picture). Excellent oxygen activation and high catalytic activity in the oxidation of formaldehyde was observed.

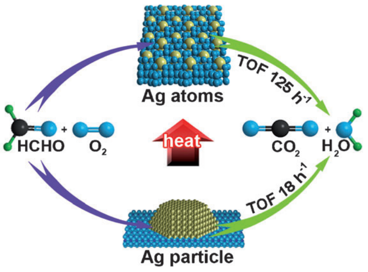

Structure Elucidation

D. Globisch, C. A. Lowery, K. C. McCague, K. D. Janda* ______ **4204 – 4208**

Uncharacterized 4,5-Dihydroxy-2,3-Pentanedione (DPD) Molecules Revealed Through NMR Spectroscopy: Implications for a Greater Signaling Diversity in Bacterial Species

Inside Back Cover

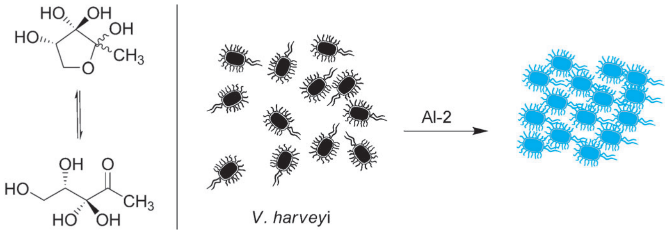

Talking bacteria: The combination of NMR spectroscopy and 4,5-dihydroxy-2,3-pentanedione (DPD) homologue analysis reveals that DPD, a bacterial signaling compound in the autoinducer-2 (AI-2) class (see scheme), exists as a much more complex structural array of molecules than previously appreciated. This finding suggests the existence of a larger bacterial chemical signaling language than previously thought.

Catalysis

S. Wang, L. Zhang, Z. Xia, A. Roy, D. W. Chang, J.-B. Baek, L. Dai* ______ **4209 – 4212**

BCN Graphene as Efficient Metal-Free Electrocatalyst for the Oxygen Reduction Reaction

A facile approach has been developed to prepare B,N co-doped graphene with tuneable composition simply by thermal annealing graphene oxide in the presence of boric acid and ammonia. The resultant BCN graphene (see picture; C gray, H white, B pink, N blue) has superior electrocatalytic activity over commercial Pt/C electrocatalysts for the oxygen reduction reaction in alkaline media.

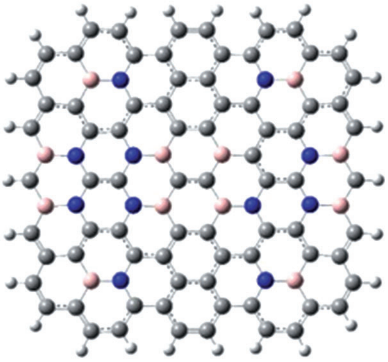

Zeolites

J. Zečević, C. J. Gommes, H. Friedrich, P. E. de Jongh, K. P. de Jong* ______ **4213 – 4217**

Mesoporosity of Zeolite Y: Quantitative Three-Dimensional Study by Image Analysis of Electron Tomograms

Quantitative insight into the three-dimensional morphology of complex zeolite Y mesopore networks was achieved by combining electron tomography and image processing. Properties could be studied that are not measurable by other techniques, such as the size distribution of the intact microporous domains. This has great relevance in descriptions of the molecular diffusion through zeolite crystals and, hence, catalytic activity and selectivity.

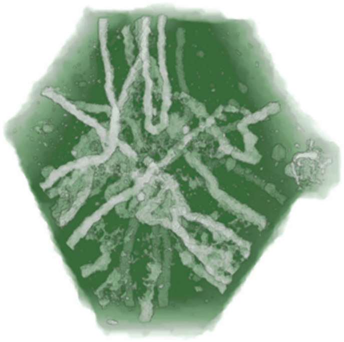

Asymmetric Aldol Reaction

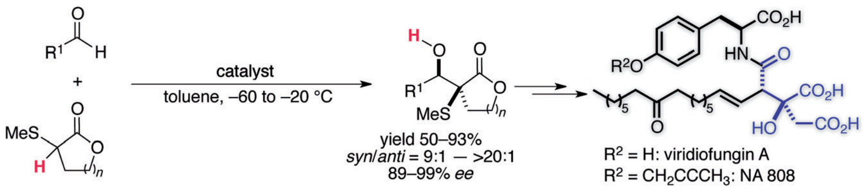

Softly does it: The title reaction, catalyzed by a $AgPF_6$/(*R*)-biphep-type ligand/DBU complex, is described (see scheme). This protocol gives efficient access to *syn*-configured α-sulfanyl-β-hydroxy lactones in a highly enantioselective manner. In one particular case, the sulfide group was stereospecifically replaced with a hydroxy group to afford an enantioenriched tertiary alcohol, which upon further manipulation led to a class of densely functionalized SPT inhibitors.

Molecular Devices

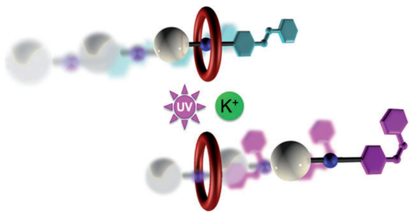

One-way path: A non-symmetric molecular axle threads a crown ether ring and is subsequently expelled along the same threading direction upon application of photochemical and chemical stimuli. The system relies on tailor-made control of the thermodynamic and kinetic properties of the system according to a flashing ratchet mechanism.

NMR Spectroscopy

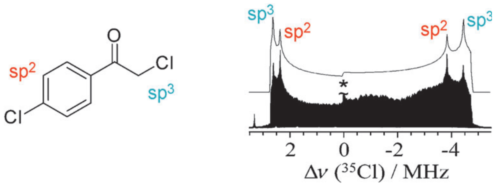

QUEST for chlorine: The chemical shifts and quadrupolar asymmetry parameters obtained from solid-state ^{35}Cl NMR spectroscopy can be related to the nature of the Cl–C bond (see picture) and to the crystal packing environment of Cl atoms that are covalently bound to carbon atoms. A method for the exact calculation of the NMR spectra, named QUEST, was developed and used for the analysis of seven different compounds.

Nanoparticles

Metallized scaffolds: Oligoproline scaffolds that are functionalized with aldehyde groups have been shown to control the size of silver nanoparticles that are formed in the Tollens reaction. The size of the nanoparticles correlates linearly with the length of the scaffold and the oxidation of the aldehyde moieties during the reaction helps to stabilize the nanoparticles through coordination to the newly formed carboxylic acid groups.

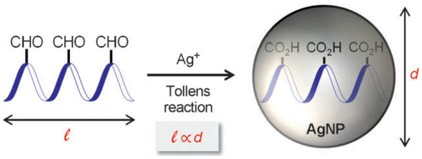

Supporting information is available on www.angewandte.org (see article for access details).

A video clip is available as Supporting Information on www.angewandte.org (see article for access details).

This article is available online free of charge (Open Access).

This article is accompanied by a cover picture (front or back cover, and inside or outside).

Service